



Cite this: *Dalton Trans.*, 2020, **49**, 1393

Received 19th November 2019,
Accepted 8th January 2020

DOI: 10.1039/c9dt04462k

rsc.li/dalton

Novel phthiocol-based organometallics with tridentate coordination motif and their unexpected cytotoxic behaviour†

Heiko Geisler,^a Debora Wernitznig,^a Michaela Hejl,^a Natalie Gajic,^a Michael A. Jakupec,^{a,b} Wolfgang Kandioller^{a,b} and Bernhard K. Keppler^{a,b}

Novel phthiocol-based organometallics with *in situ* formed tridentate N,O,O-coordination motif were established via three-component microwave assisted one-pot reaction. These complexes exhibited enhanced stability in aqueous solution compared to the parental compound KP2048 and showed unexpected cytotoxic behaviour and selectivity in 2D and 3D cell cultures.

Ruthenium arene complexes have shown promising anticancer activities *in vitro* and *in vivo* and numerous examples with different coordination motifs with various mono or bidentate ligand scaffolds, arenes and leaving groups have been reported in the literature.^{1–4} Attaching bioactive ligands to metal centres is an interesting approach for the development of metallodrugs with different modes of action compared to the ‘classical’ platinum-based anticancer agents.⁵ Quinones, especially 1,4-naphthoquinones, feature several intriguing characteristics, such as antibacterial, antiallergic, antifungal and antiviral, and thus were studied intensively over the last decades.⁶ The antitumor activity of naphthoquinones arises from the participation in cellular redox cycling and the generation of reactive oxygen species (ROS), which can lead to the oxidation of proteins, lipids, DNA or activate signalling pathways.⁶ We have recently shown that coordination of quinones (lapachol or phthiocol) with transition metals (Ru(II), Os(II) or Rh(III)) provided coordination compounds with enhanced cytotoxicity in several cancer cell lines.^{7,8} In particular, the phthiocol-based ruthenium complex **1** (KP2048; Fig. 1) showed promising results *in vitro* and *in vivo*. However, intraperitoneal treatment of mice with KP2048 led to severe side effects, such as

stiff and swollen intestines, growth of the liver, spleen and stomach, due to the local extensive reactivity.⁷ UV-Vis measurements of compound **1** in phosphate-buffered saline (PBS) solution revealed that this complex is prone to decomposition under physiological conditions (see Fig. S28 and S29†). These findings explain the extensive reactivity of this species as the complex is hydrolysed quickly, followed by ligand cleavage.

Consequently, its lack of stability is responsible for its undesired local reactivity. Hence, the complex stability was improved by insertion of a pH-dependent leaving group coupled to poly(organo)phosphazenes.⁷ Thereby, an improved cellular uptake and accumulation into tumour cells could be achieved. Promising results in *in vivo* experiments substantiated the necessity of more stable leaving groups, in order to improve the complex stability and its activity in tumour cells. Within this work various primary amines (*e.g.*, *n*-propylamine), secondary amines (morpholine, diisopropylamine), pyridines (pyridine, picoline), 1,3-diazoles (1*H*-imidazole, 1-methyl-1*H*-imidazole, 1*H*-benzimidazole) and 1,2-diazoles (1*H*-pyrazole (HPz), 1*H*-indazole (HInd), 4-methyl-1*H*-pyrazole (4-MeHPz), 4-amino-1*H*-pyrazole (4-NH₂-HPz)⁹ and 6-amino-1*H*-indazole (6-NH₂-HInd)) were attempted to replace the labile chloride leaving group.

The first experiments were performed according to literature procedures: firstly, the well-established synthesis of a di-substituted precursor complex followed by complexation with phthiocol **L** and a base (see Schemes S1 and S2†),^{10,11} and sec-

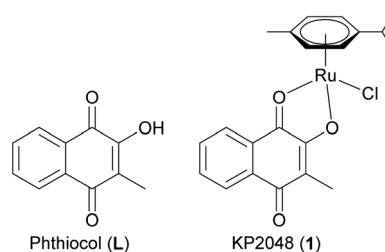


Fig. 1 2-Hydroxy-1,4-naphthoquinone **L** and phthiocol-based ruthenium cymene complex KP2048 (**1**).

^aUniversity of Vienna, Faculty of Chemistry, Institute of Inorganic Chemistry, Waehringer Str. 42, A-1090 Vienna, Austria.

E-mail: wolfgang.kandioller@univie.ac.at; Tel: +43 1 4277 52609

^bResearch Cluster ‘‘Translational Cancer Therapy Research’’, University of Vienna, Waehringer Str. 42, A-1090 Vienna, Austria

† Electronic supplementary information (ESI) available: Syntheses of the complexes, NMR characterization, stability studies *via* UV/Vis, crystallographic data. CCDC 1955180–1955187. For ESI and crystallographic data in CIF or other electronic format see DOI: 10.1039/c9dt04462k



only, the use of silver salts to form the aqua complex, and introduction of the desired *N*-containing ligand.¹² However, successful complexation was only observed with 1,2-diazoles. Unexpectedly, formation of a new tridentate ligand scaffold coordinated to the organometallic fragment took place, where a hemiaminal bond connects the naphthoquinone and the N1 nitrogen of the azole moiety (see Scheme 1). Thus, these complexes feature an additional five-membered ring between the metal centre, the oxygen (O1), the quaternary carbon (C1) and the two nitrogens of the 1,2-diazole moiety. Furthermore, these complexes exhibit two chirality centres, one at the C1 carbon which connects the pyrazole ring, the metal centre and the naphthoquinone and the second one at the metal centre itself. Due to the prevalent structure of these complexes, only two enantiomers can be formed (R_{C1}, R_{Ru} and S_{C1}, S_{Ru}). Moreover, this *in situ* formation also appeared in the case of Os(II) as metal centre; however, Rh(III) and Ir(III) did not provide complexes with this tridentate coordination motif. After the preferential formation of a tridentate ligand was observed, it was possible to establish a straightforward three-component microwave synthesis. The improved stability due to the lack of a labile chlorido leaving group allows purification by column chromatography. All complexes (**1a–e**, **2a–c**) could be synthesised *via* this one-pot reaction, where the respective dimer ($[RuCl_2(p\text{-cymene})]_2$ ¹³ or $[OsCl_2(p\text{-cymene})]_2$ ¹⁴), phthiocol (**L**)^{15,16} and 1,2-diazole (**HPz**, **HInd**, **4MeHPz**, **4-NH₂-HPz**,⁹ **6-NH₂-HInd**) were stirred in the presence of a base (NaOMe or NEt₃) under microwave irradiation for 6–12 minutes at 50–60 °C and purified *via* column chromatography using a ternary eluent system (EtOAc/*n*-hex/NEt₃ or EtOAc/MeOH/NH₄OH) in moderate to good yields (41–84%).

Formation and purity of the complexes were confirmed by 2D-NMR spectroscopy and elemental analysis (see Fig. S1–17†).

The ¹³C-NMR spectra of the complexes contain a signal around 90 ppm with low intensity, which approves the hemiaminal bond of the tridentate ligand. Additionally, single crystals of all complexes were obtained by vapour-diffusion (**1c**, **d**, **2a** and **2c**) or liquid-liquid-diffusion (**1a,b** and **2b**) from dichloromethane/diethyl ether or ethyl acetate/*n*-hexane (see Fig. S18–S27 and Tables S1–S17†). Complexes **1b**, **1c** and **2b** crystallised in the triclinic space group $P\bar{1}$. Complexes **1a** (Fig. 2), **1d**, **1e**, **2a** and **2c** crystallise in the monoclinic space groups $C2/c$, $P2_1/n$ and $P2_1/c$. Complexes containing tridentate ligands feature decreased bond lengths between O1 and the metal centre (0.05–0.090 Å), compared to compound **1**, whereas the bond length of O2–M elongated slightly (max. 0.04 Å). The bond length between the metal centre and the chlorido leaving group of complex **1** is 2.403 Å, which is considerably longer than the nitrogen-metal bond (2.078–2.116 Å) for these novel complexes.

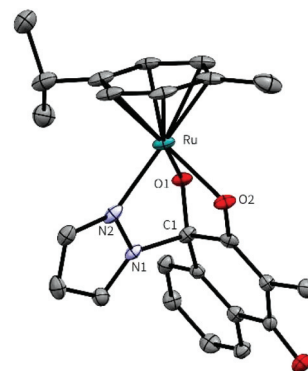
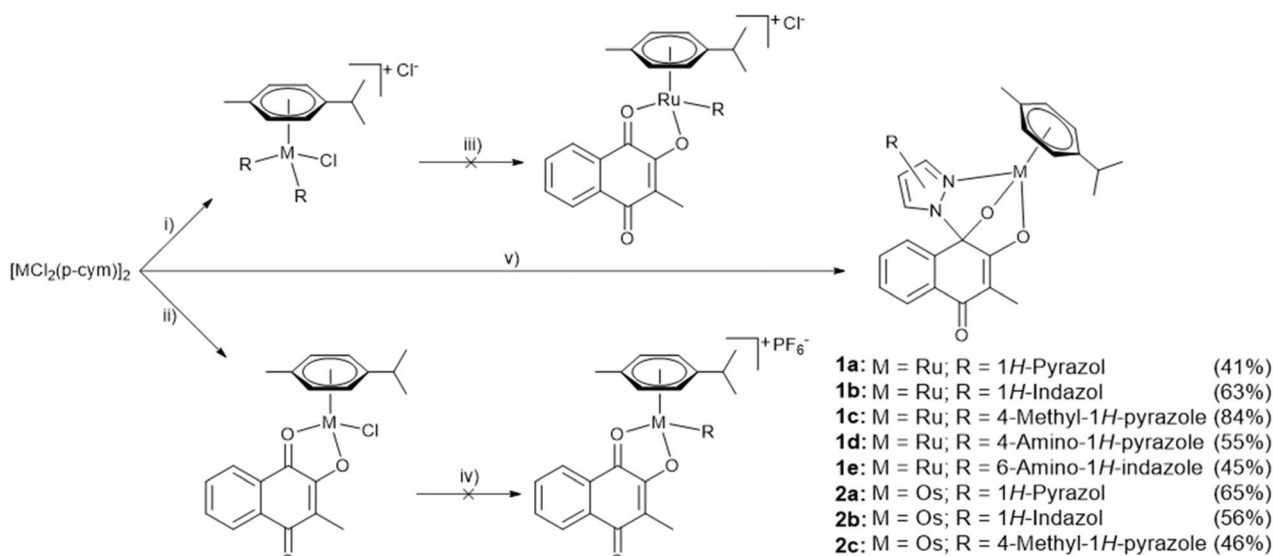


Fig. 2 Molecular structure of complex **1a** (M = Ru, R = HPz) at a 50% probability level. Hydrogens and solvent molecules were omitted for clarity.



Scheme 1 Synthetic pathway for complex synthesis; R = *N*-containing ligand; M = Ru, Os; (i) *i*-PrOH, R, microwave, 2 minutes, 60 °C; (ii) MeOH, 40 °C, phthiocol L, NaOMe, (iii) MeOH, 40 °C, phthiocol L, NaOMe; (iv) MeOH, AgPF₆, r.t.; (v) MeOH, R, phthiocol L, NaOMe/NEt₃, microwave, 50–60 °C, 6–12 minutes.



The stability of the organometallic complexes in aqueous solution (PBS, pH = 7.4, 25 °C) was determined by UV/Vis spectroscopy. Due to their poor solubility in aqueous media, 1% DMF (**1**) or DMSO (**1a–e**, **2a–c**) was used as solubilizer. Minor changes in the absorption curve of compound **1** and subsequent comparison to the free ligand (**L**) spectrum revealed a rapid degradation of complex **1** in aqueous solution (see Fig. S28 and S29†). Nevertheless, complexes **1a–2c** possess improved stability at pH 7.4, which is indicated by only small changes of the respective absorption curves over time (see Fig. S30–35†) compared to the immediate cleavage of KP2048 under these conditions. Due to presence of the hemiaminal structural feature, experiments were performed to elucidate the impact of the pH value on the aquation rate of these complexes. However, only minor changes with regard on the reaction kinetics were observed for complex **1a** under these conditions (pH 5.8–7.9, see Fig. 3 and Fig. S36–S40†).

The cytotoxic behaviour of the complexes **1a–2c** was examined with the obtained mixture of stereoisomers (R_{C1} , R_M and S_{C1} , S_M) by the colorimetric MTT assay in the human cancer cell lines CH1/PA-1 (ovarian teratocarcinoma), SW480 (colon carcinoma) and A549 (non-small cell lung carcinoma). The building blocks of the complexes, phthiocol **L**, azoles (see Table S18†) and dimeric metal precursors showed no relevant cytotoxic activities. Compound **1** with chlorido as leaving group exhibited increased cytotoxicity compared to the free ligand phthiocol **L**. However, introduction of the tridentate N,O,O coordination motif dramatically changed the cytotoxic properties of the complexes. Overall the developed complexes exhibited cytotoxic potencies down to the low nanomolar range in SW480 (IC_{50} values: 0.057–5.5 μ M) and A549 (IC_{50} values: 0.91–47 μ M) cancer cells, with ruthenium compounds being slightly more active than their osmium analogues (Table 1, Fig. S41 and S42†).

Conversely, cytotoxic potencies of these compounds are surprisingly reduced in the cancer cell line CH1/PA-1 (IC_{50} values: 40–119 μ M), although these cells have shown to be highly sen-

Table 1 *In vitro* anticancer activity (mean IC_{50} values \pm standard deviations from the MTT assay, exposure time: 96 h) of complexes **1a–2c** compared with compound **1**, phthiocol **L**, cisplatin and KP1339/BOLD-100 in monolayer cultures of three human cancer cell lines

IC_{50}/μ M	IC_{50}/μ M		
	A549	SW480	CH1/PA-1
L	210 \pm 32	116 \pm 37	129 \pm 29
1 (KP2048) ⁷	47 \pm 4	15 \pm 3	31 \pm 10
1a	1.2 \pm 0.2	0.094 \pm 0.031	>50
1b	0.91 \pm 0.10	0.057 \pm 0.008	40 \pm 4
1c	2.1 \pm 0.6	0.17 \pm 0.04	119 \pm 25
1d	47 \pm 10	5.5 \pm 1.5	62 \pm 4
1e	5.4 \pm 1.0	0.62 \pm 0.06	102 \pm 16
2a	7.4 \pm 0.3	0.26 \pm 0.03	>100
2b	3.2 \pm 0.3	0.16 \pm 0.03	61 \pm 7
2c	13 \pm 3	0.49 \pm 0.13	117 \pm 3
Cisplatin ¹⁷	6.2 \pm 1.2	3.3 \pm 0.2	0.077 \pm 0.006
KP1339/BOLD-100 ¹⁸	156 \pm 11	88 \pm 19	62 \pm 9

sitive to many coordination compounds of, *e.g.*, Ru(II), Ru(III), Os(II), Rh(III), Au(I), Ag(I), Cu(II), Pt(II), Pt(IV) and Fe(II).^{7,8,11,19–22} In contrast, the activity in the rather insensitive SW480 cells of ruthenium compounds **1a–c** is increased by at least two orders of magnitude compared to the CH1/PA-1 cell line. These results may portend to a pronounced selectivity for SW480 cells. Amino functionalised ruthenium arene complexes **1e**, **1d** revealed improved aqueous solubility; however, cytotoxicity was lowered up to 60 times depending on the cell line. Therefore, it can be assumed that the antiproliferative activity critically depends on the azole moiety. The cytotoxic potencies of **1a,b** in the cancer cell line SW480 are comparable with the currently most active organoruthenium complexes reported by Süß-Fink and co-workers (with IC_{50} values down to 30 nM in A2780 and A2780cisR cells).^{23,24} The only other reported Ru(II) arene complexes bearing a tridentate ligand scaffold were based on a N,N,N coordination motif (diethylenetriamine) and found to be nearly inactive. It was assumed that this behaviour arises from the lack of a labile leaving group, which leads to inertness against ligand exchange reactions such as aquation and therefore prevents biomolecule interactions.²⁵

The compounds were also tested for their anticancer activity in four different human cancer cell lines grown as multicellular spheroids with an exposure time of 96 h (Fig. 4). These 3D models provide more information about the cytotoxic behaviour of the compounds, since spheroids are able to

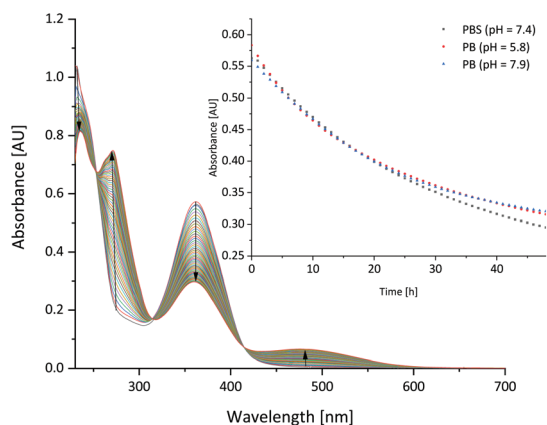


Fig. 3 Left: Absorption curves of compound **1a** over 48 h in PBS (pH = 7.2; 25 °C). Right: Absorption vs. time at 363 nm at different pH values (5.8–7.9).

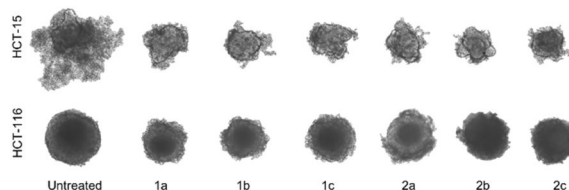


Fig. 4 Representative images of HCT-15 and HCT-116 multicellular spheroids treated with novel complexes at about the respective IC_{50} for 96 h, compared to untreated controls.



mimic the main properties of human solid tumours.²⁶ It is known from the literature that the enhanced *in vitro* activity of some metal-based compounds in 2D monolayers is dramatically reduced when the experiments are performed using 3D models.²⁷ They displayed varying cytotoxic potencies depending on the cell line. Interestingly, all compounds were very active in the usually more 'resistant' cell lines A-549, HCT-15 and HCT-116. The surprisingly low IC₅₀ values obtained in the three-dimensional *in vitro* model are listed in Table 2. These results are in good agreement with the obtained 2D data and confirm the unexpected activity in more chemo-resistant human cancer cell lines. Further studies are necessary and ongoing to explain the mechanisms underlying the resistance of the CH1/PA-1 cell line to these compound class, which lead to the major differences in the IC₅₀ values compared to the other three cell lines. Additionally, the CH1/PA-1 cell line might represent a valuable tool, which might support the understanding of the actual mode of action of this compound class.

To the best of our knowledge we report on the first examples of highly cytotoxic tridentate *N,O,O*-coordinated M(arene) complexes, which were synthesised *via* a three-component one-pot reaction under microwave conditions. The formation and purity of the compounds was confirmed by standard analytical methods. The improved stability compared to the parental complex KP2048 was proved by UV/Vis measurements under physiologically relevant conditions. Besides the enhanced stability, the introduction of the 1,2-diazole moiety allows further fine-tuning of pharmacokinetic properties, due to the broad range of feasible modifications at this site. It was found that this compound class, although designed as prodrugs for KP2048, is not activated by transformation to this species under acidic conditions and this reflects in a different cytotoxicity profile *in vitro*. The complexes displayed a remarkably high activity in the usually rather insensitive human cancer cell lines SW480 and A549 with IC₅₀ values down to 57 nM, which is in the same range as the most potent organoruthenium complexes reported so far. Surprisingly, these organometallics show no relevant cytotoxicity in the chemo-sensitive cell line CH1/PA-1. The same trend was observed in a variety of multicellular tumour spheroid models,

where also pronounced cytotoxic activities were observed in those grown from more chemo-resistant cell lines.

However, further experiments are necessary and currently ongoing to clarify the observed highly unexpected cytotoxic behaviour.

Conflicts of interest

There are no conflicts to declare.

Notes and references

- 1 Y. K. Yan, M. Melchart, A. Habtemariam and P. J. Sadler, *Chem. Commun.*, 2005, 4764–4776, DOI: 10.1039/b508531b.
- 2 G. Suss-Fink, *Dalton Trans.*, 2010, **39**, 1673–1688.
- 3 L. Zeng, P. Gupta, Y. Chen, E. Wang, L. Ji, H. Chao and Z. S. Chen, *Chem. Soc. Rev.*, 2017, **46**, 5771–5804.
- 4 T. Bugarcic, A. Habtemariam, R. J. Deeth, F. P. Fabbiani, S. Parsons and P. J. Sadler, *Inorg. Chem.*, 2009, **48**, 9444–9453.
- 5 K. J. Kilpin and P. J. Dyson, *Chem. Sci.*, 2013, **4**, 1410–1419.
- 6 K. W. Wellington, *RSC Adv.*, 2015, **5**, 20309–20338.
- 7 C. M. Hackl, B. Schoenhacker-Alte, M. H. M. Klose, H. Henke, M. S. Legina, M. A. Jakupec, W. Berger, B. K. Keppler, O. Brüggemann, I. Teasdale, P. Heffeter and W. Kandioller, *Dalton Trans.*, 2017, **46**, 12114–12124.
- 8 W. Kandioller, E. Balsano, S. M. Meier, U. Jungwirth, S. Göschl, A. Roller, M. A. Jakupec, W. Berger, B. K. Keppler and C. G. Hartinger, *Chem. Commun.*, 2013, **49**, 3348–3350.
- 9 C. Maccallini, M. Di Matteo, D. Vullo, A. Ammazalorso, S. Carradori, B. De Filippis, M. Fantacuzzi, L. Giampietro, A. Pandolfi, C. T. Supuran and R. Amoroso, *ChemMedChem*, 2016, **11**, 1695–1699.
- 10 M. Schmidlehner, P.-S. Kuhn, C. M. Hackl, A. Roller, W. Kandioller and B. K. Keppler, *J. Organomet. Chem.*, 2014, **772–773**, 93–99.
- 11 C. M. Hackl, M. S. Legina, V. Pichler, M. Schmidlehner, A. Roller, O. Domotor, E. A. Enyedy, M. A. Jakupec, W. Kandioller and B. K. Keppler, *Chemistry*, 2016, **22**, 17269–17281.
- 12 C. A. Riedl, M. Hejl, M. H. M. Klose, A. Roller, M. A. Jakupec, W. Kandioller and B. K. Keppler, *Dalton Trans.*, 2018, **47**, 4625–4638.
- 13 S. B. Jensen, S. J. Rodger and M. D. Spicer, *J. Organomet. Chem.*, 1998, **556**, 151–158.
- 14 W. A. Kiel, R. G. Ball and W. A. G. Graham, *J. Organomet. Chem.*, 1990, **383**, 481–496.
- 15 L. Kathawate, S. P. Gejji, S. D. Yeole, P. L. Verma, V. G. Puranik and S. Salunke-Gawali, *J. Mol. Struct.*, 2015, **1088**, 56–63.
- 16 R. Zhu, L. Xing, X. Wang, C. Cheng, B. Liu and Y. Hu, *Synlett*, 2007, 2267–2271.
- 17 H. P. Varbanov, S. Goschl, P. Heffeter, S. Theiner, A. Roller, F. Jensen, M. A. Jakupec, W. Berger, M. Galanski and

Table 2 Comparison of IC₅₀ values (means ± standard deviations from the AlamarBlue assay) of compounds **1a–c** and **2a–c** after 96 h of incubation in multicellular tumour spheroids grown from four human cancer cell lines

IC ₅₀ /μM				
	A549	HCT-15	HCT-116	CH1/PA-1
1a	4.6 ± 3.1	0.97 ± 0.43	0.67 ± 0.27	50 ± 8
1b	5.1 ± 3.1	0.74 ± 0.45	0.95 ± 0.28	118 ± 9
1c	1.4 ± 0.2	0.99 ± 0.09	1.4 ± 0.3	95 ± 10
2a	15 ± 1	1.8 ± 0.5	21 ± 3	>400
2b	8.2 ± 1.2	1.6 ± 0.5	15 ± 1	135 ± 10
2c	17 ± 2	4.5 ± 1.1	31 ± 4	>400



- B. K. Keppler, *J. Med. Chem.*, 2014, **57**, 6751–6764.
- 18 P. S. Kuhn, V. Pichler, A. Roller, M. Hejl, M. A. Jakupec, W. Kandioller and B. K. Keppler, *Dalton Trans.*, 2015, **44**, 659–668.
- 19 H. P. Varbanov, M. A. Jakupec, A. Roller, F. Jensen, M. Galanski and B. K. Keppler, *J. Med. Chem.*, 2013, **56**, 330–344.
- 20 M. F. Primik, S. Goschl, M. A. Jakupec, A. Roller, B. K. Keppler and V. B. Arion, *Inorg. Chem.*, 2010, **49**, 11084–11095.
- 21 M. J. McKeage, P. Papathanasiou, G. Salem, A. Sjaarda, G. F. Swiegers, P. Waring and S. B. Wild, *Met.-Based Drugs*, 1998, **5**, 217–223.
- 22 A. Houlton, R. M. G. Roberts and J. Silver, *J. Organomet. Chem.*, 1991, **418**, 107–112.
- 23 A. P. Basto, J. Muller, R. Rubbiani, D. Stibal, F. Giannini, G. Suss-Fink, V. Balmer, A. Hemphill, G. Gasser and J. Furrer, *Antimicrob. Agents Chemother.*, 2017, **61**.
- 24 F. Giannini, J. Furrer, A. F. Ibao, G. Suss-Fink, B. Therrien, O. Zava, M. Baquie, P. J. Dyson and P. Stepnicka, *J. Biol. Inorg. Chem.*, 2012, **17**, 951–960.
- 25 M. V. Babak, S. M. Meier, A. A. Legin, M. S. Adib Razavi, A. Roller, M. A. Jakupec, B. K. Keppler and C. G. Hartinger, *Chemistry*, 2013, **19**, 4308–4318.
- 26 A. S. Nunes, A. S. Barros, E. C. Costa, A. F. Moreira and I. J. Correia, *Biotechnol. Bioeng.*, 2019, **116**, 206–226.
- 27 E. Schreiber-Brynzak, E. Klapproth, C. Unger, I. Lichtscheidl-Schultz, S. Goschl, S. Schweighofer, R. Trondl, H. Dolznig, M. A. Jakupec and B. K. Keppler, *Invest. New Drugs*, 2015, **33**, 835–847.

